Modulation of Interaction Forces Between Bilayers Exposing Short-Chained Ethylene Oxide Headgroups

T. L. Kuhl, D. E. Leckband, D. D. Lasic, and J. N. Israelachvili
Department of Chemical and Nuclear Engineering, University of California, Santa Barbara, California 93106, and Liposome Technology, Inc., Menlo Park, California 94025 USA

ABSTRACT The use of liposomes as drug delivery systems has been limited by their rapid clearance from circulation by the mononuclear phagocyte system. Recent studies have found that circulation times can be greatly enhanced by incorporating a small amount of modified lipids whose headgroups are derivatized with a bulky water soluble polymeric chain of poly ethylene oxide. We report here a systematic study using the Surface Forces Apparatus to measure directly the interactions between two phosphatidyl ethanolamine lipid bilayers, exposing this polymeric headgroup at different concentrations in the bilayer. We found that the force becomes repulsive at all separations and that the thickness of the steric barrier could be controlled easily by adjusting the concentration of the modified lipids. Equilibrium force profiles were measured that were reversible and largely insensitive to changes in electrolyte concentration and temperature. The results have enabled the Dolan and Edwards theory for the steric forces of low coverage polymer surfaces and the Alexander de Gennes theory for high coverage surfaces to be tested, and both were found to apply. We conclude that these simple theories can be used to model the interactions of surprisingly short segments and, hence, apply to such systems as lipids with bulky headgroups and liposomes containing a sterically stabilizing polymer.

INTRODUCTION

The presence of terminally grafted polymers at the particle-solution interface of colloidal particles and biomaterials is currently receiving considerable attention, especially regarding sterically stabilized liposomes and vesicles used for drug delivery (Woodle and Lasic, 1992). It has already been experimentally established that the grafting of water soluble polymers like PEO dramatically enhances the circulation time of liposomes from a few hours to days in vivo (Klibanov et al., 1990; Lasic et al., 1991; Allen et al., 1991a, b; Papahadjopoulos et al., 1991). The enhanced circulation time is believed to be due to steric stabilization of the liposomes by the grafted polymer, preventing their close approach to cellular surfaces in the body, which is necessary to prevent adhesion, fusion, lysis, or destruction of the liposomes by the immune system. In addition, the special properties of PEO such as chemical inertness, biocompatibility, water solubility, insensitivity to changes in solution ionic conditions due to its nonionic character, and low protein adsorption have made it a particularly suitable polymer for use as a steric stabilizer in aqueous media including body fluids (Woodle and Lasic, 1992; Golander et al., 1992; Blume and Cevc, 1990).

Needham and colleagues (Needham et al., 1992a, b) recently reported that the polymeric group acts as a steric barrier increasing the repulsion between oriented multilayers and unoriented multiwalled liposomes. It is believed that the steric barrier of the ethylene oxide group and its biocompatibility results in the extended circulation times found in vivo (Needham et al., 1992a, b). A number of papers have been published exploring the behavior of such systems and their potential applications (Woodle and Lasic, 1992; Klibanov et al., 1990; Lasic et al., 1991; Allen et al., 1991a, b; Papahadjopoulos et al., 1991).

This work presents the results of detailed measurements showing how the forces between supported lipid bilayers of double-chained zwitterionic lipids in aqueous solutions are modified by the attachment of poly ethylene oxide chains. Unlike most of the polymer systems that have been investigated to date, the ethylene oxide (EO) chains here were covalently bound to the headgroup of distearoyl phosphatidyl ethanolamine (DSPE), thereby forming the surfactant-polymer DSPE-EO_{45} (Fig. 1). The PEO chains have a molecular weight of 2000 (45 monomers, $R_F = 35$ Å) and a polydispersity of 1.1. These are very short chains, and, therefore, the modified DSPE-EO_{45} molecules may also be considered as lipids or surfactants having an extra large hydrophilic headgroup.

One aim of looking at low M_r polymers or short chains is to test the limits of polymer scaling theories. Another is to establish a link with the interactions of normal surfactant or lipid monolayers/bilayers and those having many flexible segments in their headgroups, for example, gangliosides, glycolipids, sugars, polysaccharides, etc. On the practical side, the effective steric stabilization of many colloidal particles, especially vesicles and liposomes, is more likely to be accomplished by short chains than by highly hysteretic and less economical long-chain polymers.

The system studied was composed of two interacting bilayers prepared by Langmuir-Blodgett (LB) deposition. The

---

Received for publication 22 October 1993 and in final form 14 February 1994.

Address reprint requests to Jacob N. Israelachvili, Department of Chemical and Nuclear Engineering, University of California-Santa Barbara, Santa Barbara, CA 93106-5080. Tel.: 805-893-8407/3412; Fax: 805-893-4731.

0006-3495/94/05/1479/10 $2.00

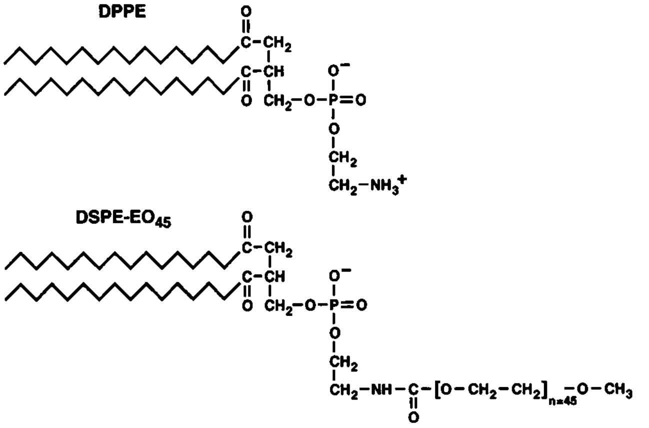

FIGURE 1 Structure of the zwitterionic lipid DPPE and the modified lipid DSPE-EO$_{45}$. Notice that DSPE-EO$_{45}$ is negatively charged.

outer bilayer surface was composed of a mixture of unmodified DSPE the matrix lipid, doped with 1–10% DSPE-EO$_{45}$. Because the polymer is covalently bound to the DSPE headgroup, the surface coverage can be quantitatively controlled in two ways: (i) varying the mole fraction of the components (DSPE-EO$_{45}$ to DSPE), and (ii) varying the surface area occupied per molecule during the LB deposition. The actual percentages used were 1.3, 4.5, and 9.0% (mole/mole DSPE-EO$_{45}$ to DSPE). Fig. 2 shows a schematic of these three packing regimes. The DSPE molecular area was 43 Å^2 in all cases. At the lower concentration of 1.3% DSPE-EO$_{45}$, the polymer chains are not perturbed by their neighbors and are in the "mushroom" regime. The 4.5% concentration gives rise to a weakly interacting or "weak overlap" regime, whereas at 9.0%, the highest surface concentration studied, the polymer chains are strongly interacting and in the "brush" regime.

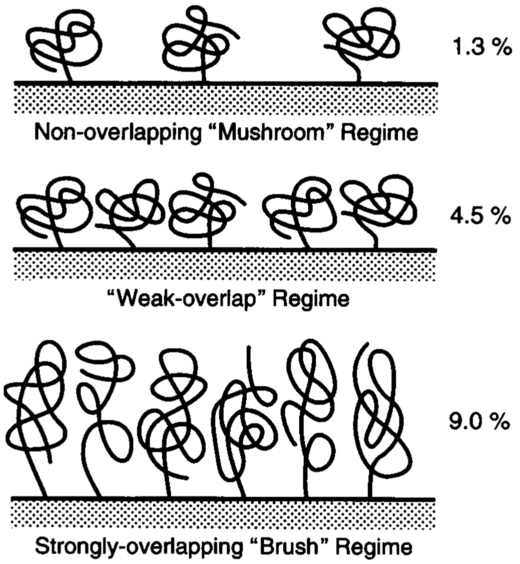

FIGURE 2 Schematic of the change in polymer layer thickness and density as a function of DSPE-EO$_{45}$ concentration in the exposed outer monolayer of the bilayer.

MATERIALS AND METHODS

Materials

High purity dipalmitoyl phosphatidyl ethanolamine (DPPE) and distearoyl phosphatidyl ethanolamine were purchased from Avanti Polar Lipids Inc. (Alabaster, AL) in powder form. Modified DSPE-EO$_{45}$ was kindly supplied by Liposome Technology Inc. (Menlo Park, CA). Potassium Nitrate (KNO$_3$) from Sigma Chemical Co. (St. Louis, MO) was used without further purification. The water was first ion exchanged, distilled in an all Pyrex still, and finally passed through a Millipore water-purification system.

Deposition of bilayers

LB deposition was used to construct supported bilayers on mica. The supported bilayers were composed of zwitterionic lipids that bind physically, but strongly to mica. The LB technique enables the packing density of the deposited lipids to be controlled (Gaines, 1969). The amphiphilic molecules orient at the air-water interface with the polar headgroups in the water sub phase and the tails jutting into the air (Fig. 3). A barrier is used to compress the molecules on the water surface to the desired packing density. At this stage a suitable substrate, in this case mica, can be drawn through the air-water interface, resulting in the transfer of the monolayer from the sub phase to the substrate.

Being hydrophilic, atomically smooth, and with an exchangeable surface charge density of one charge per ~45 Å^2, mica is particularly suitable for these studies (Parker et al., 1989). The phosphatidyl ethanolamine (PE) headgroups are zwitterionic with the positively charged amine group at the end of the headgroup binding electrostatically to the negatively charged mica surface. At their highest packing density, the PE headgroups and their two chains have a surface area of 43 Å^2, closely matching the surface lattice and charge of mica.

The first monolayer of the deposited bilayer was a close-packed DPPE monolayer at an area of about 43 Å^2 per molecule. This DPPE monolayer provides a smooth hydrophobic surface for deposition of a second monolayer (Marra and Israelachvili, 1985). Construction of the DPPE layer was done as follows. First, the mica substrate is totally immersed into the water

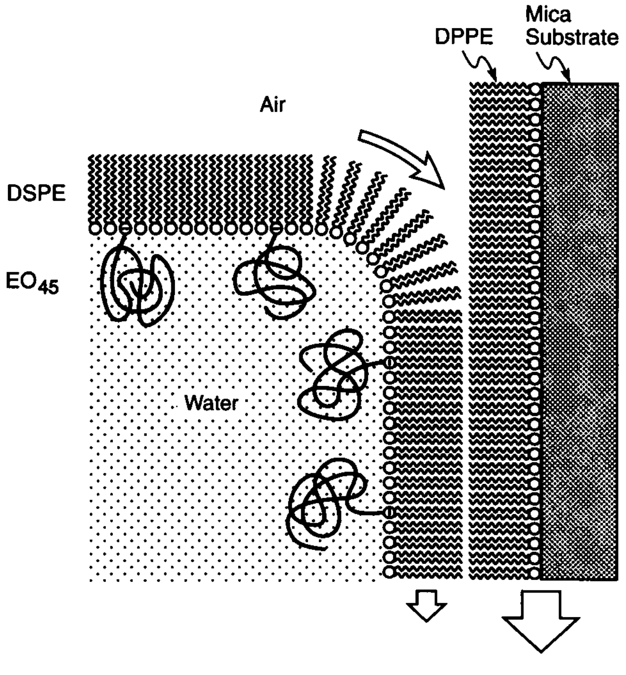

FIGURE 3 Mixed DSPE and DSPE-EO$_{45}$ monolayer at the water-air interface and deposition of the layer on the hydrophobized (DPPE) mica substrate.

sub phase of the trough. Next, DPPE is spread on the water surface, and the monolayer is compressed to a molecular area of 43 Å^2 at a surface pressure of 41 mN/m, after which the mica is slowly raised through the water-air interface at constant pressure. In this manner the DPPE is deposited on the mica surface at the same packing density as on the water surface (Marra, 1985). The second layer of DSPE, containing 1–10% DSPE-EO$_{45}$, is constructed in a similar manner, except that the DPPE modified mica surface is lowered through the air-water interface (Fig. 3). The second monolayer is physically bound to the DPPE coated mica by the hydrophobic interaction between the double-chain hydrocarbon tails of the DPPE and DSPE monolayers. Once the second layer is deposited, the substrate is kept under water because exposure of a bilayer-coated surface to air can result in removal of the outer monolayer. A schematic diagram of the bilayers constructed on mica and their positioning during the subsequent force measurements, described below, is shown in Fig. 4.

Surface pressure characterizations

Fig. 5 shows the surface pressure-area (*P-A*) curves of DSPE alone and with the various concentrations of bound PEO (1.3, 4.5, and 9.0 mol%) at 21 ± 1°C. As shown in Fig. 3, DSPE molecules at the air-water interface are expected to be oriented with the PEO chains extending into the water sub phase. As the concentration of DSPE-EO$_{45}$ to unmodified DSPE increases, the area per DSPE molecule at which a pressure is measured increases proportionally. This additional surface pressure is due to the repulsive lateral steric interaction of the PEO chains. The characteristic increase in the lateral surface pressure with increasing DSPE-EO$_{45}$ concentration correlates with normal inter-surface force measurements, as measured with the surface forces apparatus. A quantitative analysis of these correlations will be reported in a later manuscript.

Pure DSPE attains a limiting packing density of 43 Å^2 at a surface pressure of 37 mN/m (Gaines, 1969). The mixed 1.3, 4.5, and 9.0% layers were transferred at surface pressures of 39, 43, and 42 mN/m, respectively. At these pressures the DSPE layer is in the solid gel phase with an area of approximately 43 Å^2 per molecule for all three concentrations of DSPE-EO$_{45}$. These monolayers were found to be quite stable on the air-water interface, but some loss of molecules was experienced during the compression cycle. This loss was attributed to the squeezing out of contaminants, because the modified DSPE with bound PEO was 90–95% pure. Moreover, after the first compression of the monolayer, no loss of material from the interface was measured. Contaminants included unbound PEO chains, water, and salts (D. Lasic, personal communication). Finally, transfer ratios as determined with large test pieces of mica coated with DPPE were generally 1.00 ± 0.05. A transfer ratio of 1.0 suggests that the packing density of the molecules on the water surface is retained on the substrate (Marra, 1985). All depositions were carried out at 21 ± 1°C.

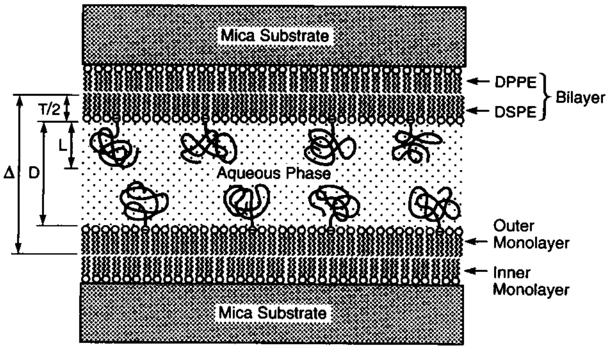

FIGURE 4 Schematic representation of the bilayer-coated mica surfaces including definition of distances, where contact is defined by $D = 0$ and $D = \Delta - T$. T is the thickness of the two outer monolayers; L is the thickness of the polymer layer, and L_0 is the anhydrous thickness of the polymer layer, i.e., under high compression, $L \rightarrow L_0$.

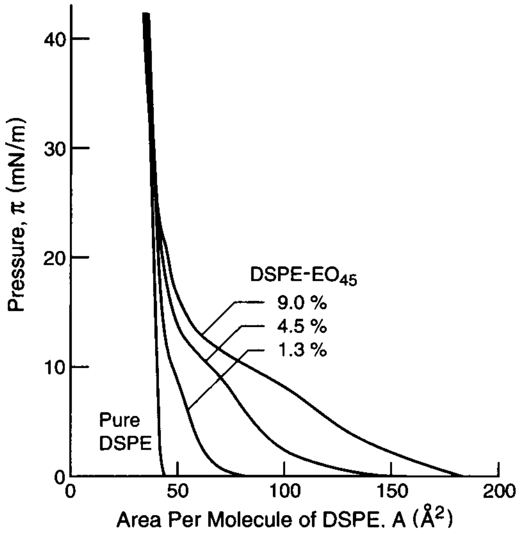

FIGURE 5 Monolayer compression (*P-A*) isotherms of pure DSPE and 1.3, 4.5, and 9.0% DSPE-EO$_{45}$ at 21 ± 1°C.

An important consideration is whether the DSPE/DSPE-EO$_{45}$ mixtures phase separate. Phase separation can be determined by comparing the collapse pressures of the DSPE/DSPE-EO$_{45}$ mixtures with those of the pure components. We found that the collapse pressures of the mixtures were in between those of pure DSPE (50 mN/m), and pure DSPE-EO$_{45}$ (65 mN/m). Further, the measured collapse pressure increased monotonically as the fraction of DSPE-EO$_{45}$ increased from 0 to 9%. These data indicate that the mixture behaves ideally or nearly so in the experimentally relevant range of compositions, which would not be the case if phase separation was occurring. Finally, we found no evidence of phase separation during any of the subsequent force measurements. Therefore, throughout this work we assume that phase separation does not occur.

Solution properties of PEO

Unlike other polyethers, PEO is water soluble at moderate temperatures in all proportions for a wide range of molecular weights. The upper consolute temperature in pure water is 118°C. The addition of monovalent and divalent salts lowers the theta temperature moderately. For example, in 400 mM divalent electrolyte solutions the theta temperature is lowered to about 42°C. Monovalent electrolyte solutions do not suppress the theta temperature as strongly (Bailey and Koleske, 1990).

PEO's unusual water solubility is believed to be the result of specific structuring with water. PEO forms helical coils in water (Kjellander and Florin, 1981) to maximize its hydrogen binding with water and to minimize the amount of exposed hydrophobic groups. There is data suggesting that two water molecules are associated with each EO monomer and that the diffusion coefficient of water near the chain is substantially lower than in bulk water (Glowinkowski et al., 1981; Liu and Parsons, 1969; Maconnachie et al., 1978). Raman Spectra of PEO in solution have shown that the chain conformation in aqueous solutions is more ordered than in organic solvents or in the pure polymer melt (Koenig and Angood, 1970). In fact, the structure closely resembles that of the helical crystalline state, with slightly more disorder in aqueous solution. One interesting aim of this study was to determine whether scaling laws for long-chain random coils apply to short polymer chains, particularly PEO with its specific, nonrandom structure in water.

Surface forces apparatus

The surface forces apparatus technique has been previously described (Israelachvili and Adams, 1978; Israelachvili, 1973). The interaction forces, both attractive and repulsive, are measured between two crossed mica sheets, which are back silvered and glued onto cylindrical silica discs. In these experiments, the mica surfaces were coated with bilayers as already described. The separation between the treated mica surfaces was measured with an optical technique based on multiple beam interference fringes (Fringes of Equal Chromatic Order, FECO). From the position of the FECO fringes in the spectrometer, the distance between the two surfaces could be measured with a resolution of 1 Å. The distance between the surfaces is controlled by a series of coarse and fine micrometers. Additional control of the separation was achieved with a piezoelectric crystal attached to the upper disc. The forces between the surfaces are measured from the deflection of a variable cantilever spring supporting the lower surface.

This technique enabled us to measure the force-distance profiles between bilayer-coated mica sheets and to investigate the thickness, compressibility, and relaxation processes occurring in PEO systems.

RESULTS

Definition of the bilayer-water interface

Before describing the results of the normalized force-distance, $F(D)/R$, measurements, it is important to establish an appropriate reference separation for the contact between the polymer-coated bilayer surfaces, which will define $D = 0$. The combined thickness of the two outer monolayers, T, together with their PEO layers, L, was determined at the end of each experiment by measuring the thickness change after drainage of the solution from the apparatus and removal of the two outer monolayers (Fig. 4). The thickness change Δ was measured relative to the distance of closest approach during the force measurements and, therefore, corresponds to the two DSPE monolayers with their bound and highly compressed polymer layer.

We define bilayer-bilayer contact, $D = 0$, as the contact between nominally dehydrated bilayers (Marra and Israelachvili, 1985) without any water or polymer layer between them (Fig. 4). Thus,

$$D = \Delta - T. \qquad (1)$$

Because the DSPE monolayers (m.p. = 74°C) were deposited at room temperature in a close packed solid phase, no phase changes or density changes are expected to take place, and the thickness of the bilayer was assumed to remain constant during experiments. Desorption of the outer monolayer was prevented by presaturation of the electrolyte solution with DSPE.

The anhydrous bilayer thickness (T) was calculated from the known volumes occupied by the hydrocarbon chains and PE headgroups and is given by $T = 2[2V_{\text{hc}} + V_{\text{head}}]/A$, where $V_{\text{hc}} = (27.4 + 26.9n)$ Å^3 is the average volume of a saturated n-carbon chain in the frozen or gel state (Tanford, 1972), $V_{\text{head}} = 243$ Å^3 is the average headgroup volume of PE (Small, 1967), and A is the deposited headgroup area. For example, the thickness of two outer DSPE monolayers deposited at $A = 43$ Å^2 per molecule is calculated to be $T = 2[2(27.4 + 26.9 \times 17) + 243]/43 = 56$ Å.

Equation 1 was used to define D from measurements of Δ in all of the experimental force-distance (F/R) plots shown in this paper. If Δ is measured at high compression, we may further assume that the polymer layer thickness, L, is close to the anhydrous thickness L_o, whence we also have

$$L_o = (\Delta - T)/2. \qquad (2)$$

Table 1 shows the three polymer layer thicknesses obtained in this way. The hypothetical anhydrous bilayer-bilayer contact without polymer is taken as $D = 0$ in all of the experimental plots.

Force measurements

In the absence of a bound polymer layer, neutral PE bilayers adhere by entering an attractive van der Waals energy minimum at D = 6–8 Å, below which repulsive hydration and protrusion forces oppose closer approach (Marra and Israelachvili, 1985). When PE bilayers contain bound PEO, the van der Waals attraction is overcome at all separations by the steric and electrostatic repulsion of the polymer chains. The electrostatic repulsion arises because the DSPE-EO$_{45}$ is potentially negatively charged (Fig. 1). This leads to a long-range electrostatic double-layer repulsion between the surfaces. An important consideration here is whether the electrostatic repulsion or the steric repulsion is responsible for the enhanced circulation times of modified liposomes in vivo. Towards this end, the determination of the plane from where the diffuse double-layer originates, the outer Helmholtz plane (OHP), or the plane that defines $D = 0$ for the double-layer forces is significant. Because the only possible source of charge is the phosphate group in the DSPE headgroup, the position of $D = 0$ is taken to be at the contact between the two bilayer surfaces without bound polymer, coinciding with the same $D = 0$ as was previously chosen for determining the thickness of the polymer layer.

With this positioning of the OHP, an analysis of the experimental data can be carried out by fitting the measured force curves to the theoretical double-layer repulsion, and attributing the difference to the steric repulsion between the polymer layers. Theoretically and experimentally, both the

TABLE 1 Areas and thicknesses of adsorbed bilayers and their corresponding polymer layer

Surface coverage of polymer (% DSPE-EO$_{45}$)	Phase state	Area deposited A	Theoretical anhydrous bilayer thickness, T	Total experimental thickness Δ	Compressed polymer thickness $2L_o$
		Å^2	Å	±2Å	±2Å
1.3	gel/frozen	43	56	67	11
4.5	gel/frozen	43	56	88	32
9.0	gel/frozen	43	56	114	58

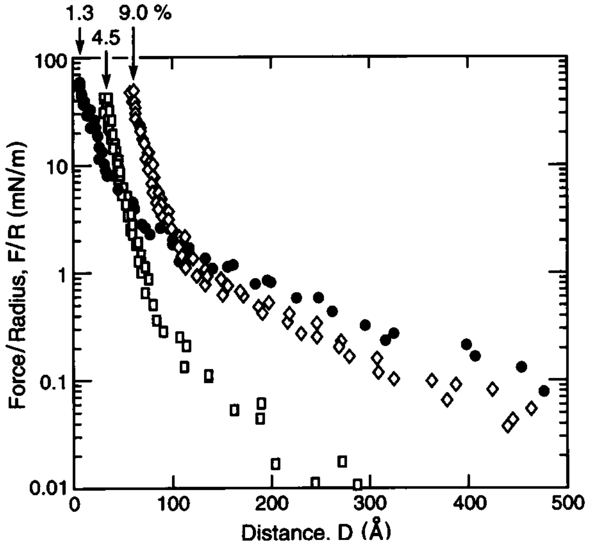

FIGURE 6 Measured force versus distance on a log plot as a function of PEO surface coverage at 21°C. The longer-ranged electrostatic repulsion extends a few hundred angstroms, whereas the steric repulsion is seen as a much steeper, and stronger, short-range repulsion. (●) Forces between bilayers containing 1.3% DSPE-EO_{45} in 0.5 mM KNO_3. (□) Forces between bilayers containing 4.5% DSPE-EO_{45} in 4.2 mM KNO_3. (◇) Forces between bilayers containing 9.0% DSPE-EO_{45} in 0.7 mM KNO_3. $D = 0$ is defined as the contact between nominally dehydrated DSPE bilayers without any polymer layer. For two cylindrically curved surfaces of radius R at a distance D apart, the force $F(D)$ between them is related to the interaction energy per unit area $E(D)$ between two planar surfaces by the Derjaguin approximation $E(D) = F(D)/2\pi R$.

electrostatic and steric forces decay roughly exponentially. In the case of electrostatic forces, the decay is determined by the ionic strength (the Debye length). For the steric interactions, the decay is determined by the thickness of the polymer layer. Unless the two decay lengths happen to be similar, a double-exponential curve is measured from which the electrostatic and steric contributions can be determined.

Fig. 6 shows a log plot of the force versus distance curves at 21°C for the three polymer surface coverages studied. The longer-ranged electrostatic repulsion extends a few hundred angstroms, whereas the steric repulsion is seen as a much steeper, and stronger, short-range repulsion. To facilitate the analysis of the steric repulsion, the electrostatic portion of the force profiles must first be subtracted. The electrostatic component of the force profile was determined by fitting the long-range (large-distance) parts of the curves to the theoretical double-layer repulsion with constant surface charge or constant surface potential boundary conditions and assuming that the dielectric constant of the medium was that of pure water, $\epsilon = 78.4$. Based on these assumptions, the electrostatic repulsion was calculated by numerically solving the nonlinear Poisson-Boltzmann equation (Grabbe, 1993).[1] The results are listed in Table 2.

TABLE 2 Electrostatic double-layer parameters

Surface coverage of polymer (% DSPE-EO_{45})	Electrolyte concentration, KNO_3	Measured Debye length κ^{-1}	Surface potential ψ_0	Surface charge density σ
	mM	Å	mV	mC/m^2
1.3	0.51	130	105	8.0
4.5	4.2	45	50	6.5
9.0	0.69	115	70	5.0

An unusual feature of the results is the trend of decreasing surface charge with increasing DSPE-EO_{45} content in the bilayer. Because the DSPE-EO_{45} headgroups are potentially negatively charged, this trend appears to be counterintuitive. However, throughout the previous analysis we have assumed that the dielectric medium was that of pure water, neglecting the effect of the ethylene oxide chains extending from the bilayer surface. Pure poly-ethylene oxide has a dielectric constant, $\epsilon = 11$, much lower than that of water (Arnold et al., 1985). Hence, as the concentration of DSPE-EO_{45} increases, the dielectric constant of the medium surrounding the charged headgroups decreases. The overall effect of this local reduction in ϵ would be: (i) a lower degree of dissociation, and (ii) a more rapid decay of the double layer potential away from the surface. Both of these effects would account for the observed trend of decreasing surface charge with increasing DSPE-EO_{45} content. A related phenomena is the well known reduction in degree of headgroup dissociation of charged surfactants from approximately 100% when dissolved as monomers in solution to approximately 25% when associated in micelles, i.e., when surrounded by the low dielectric constant environment of the hydrocarbon chains (Chen and Shen, 1990; Leckband et al., 1993)

Fig. 7 displays the best fit theoretical curves for constant surface charge and potential fitted to the asymptotic parts of the experimental force curves of Fig. 6. After subtracting the double-layer force from the total measured force, the remaining force is due only to the steric repulsion of the polymer chains. All of the data in the figures to follow have had the theoretical electrostatic repulsion (assuming constant charge) subtracted from the overall force profile. The van der Waals attraction is much smaller than either of these forces and was neglected.

Fig. 8 is a compilation of the steric force alone at 21°C after subtracting the electrostatic repulsion from the overall force curve. The steric force profile is readily seen to be a function of polymer surface coverage. In the 1.3% "mushroom" regime the forces extend ~35 Å per surface, which is the same as the Flory radius, $R_F = 35$ Å. In the 9.0% "brush" regime the polymer chains are extended significantly further from the bilayer surface, by about 65–70 Å per surface, which is twice the R_F. It is interesting to compare the 1.3% DSPE-EO_{45} noninteracting mushroom regime with the 4.5%, weakly overlapping regime. In both cases, the polymer extends about 35 Å to 40 Å per surface or one R_F, exactly the extension expected theoretically for a random coil in a good solvent (de Gennes, 1979). However, closer in, the

---

[1] The program was kindly supplied by Alexis Grabbe following the earlier work of D. Chan and R. Horn.

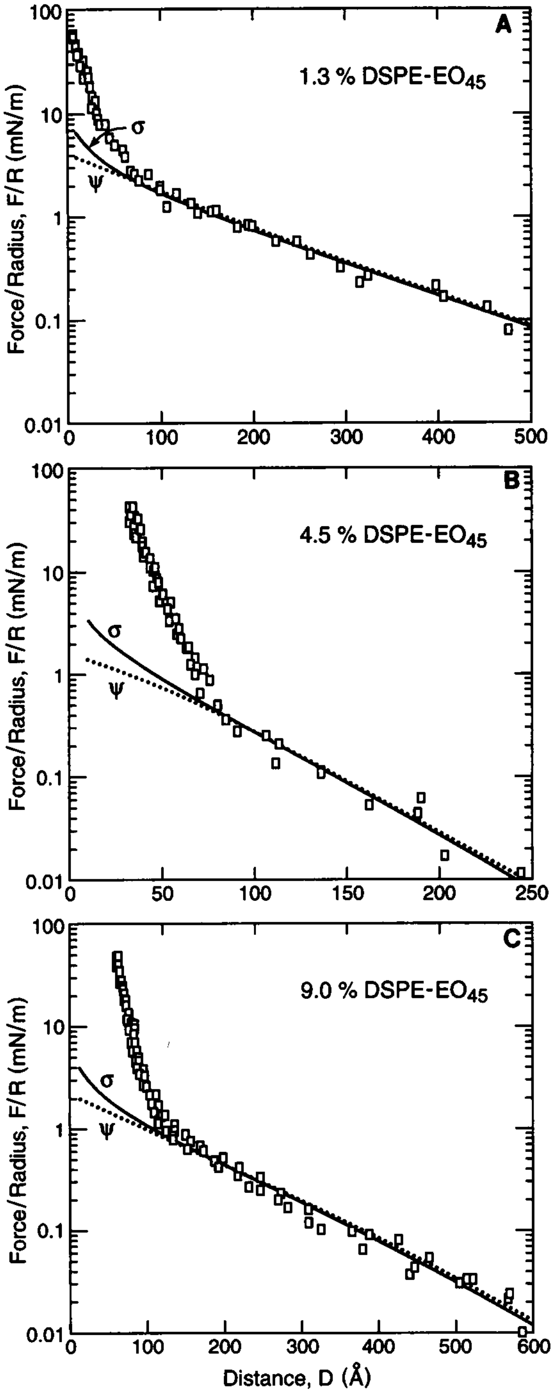

FIGURE 7 Exact numerical calculation of the theoretical double-layer repulsion with constant surface charge and constant surface potential boundary conditions fit to the data of Fig. 6. Numerical results are listed in Table 2.

layer compressibility at 1.3% coverage is much greater than that at 4.5%. This is a result of the free space available on both surfaces at 1.3% coverage as they approach for accommodating the opposing chains.

The experimental values of the packing densities and polymer layer thickness deduced for each of the PEO surface concentrations shown in Fig. 8 are listed in Table 3. From these values the projected area of a PEO chain on the bilayer surface appears to be about 900 Å^2, not 3600 Å^2 as would be deduced from $\pi R_F{}^2$. Based on this projected area of 900 Å^2 and an extension of 35 Å, the volume of a non- or weakly interacting coil is 31,500 Å^3 (area × extension). When the packing area in the 9.0% "brush" regime is used, the chains would need to extend 65 Å to attain the same coil volume and, hence, density. This is in very good agreement with the measured extension of 65–70 Å.

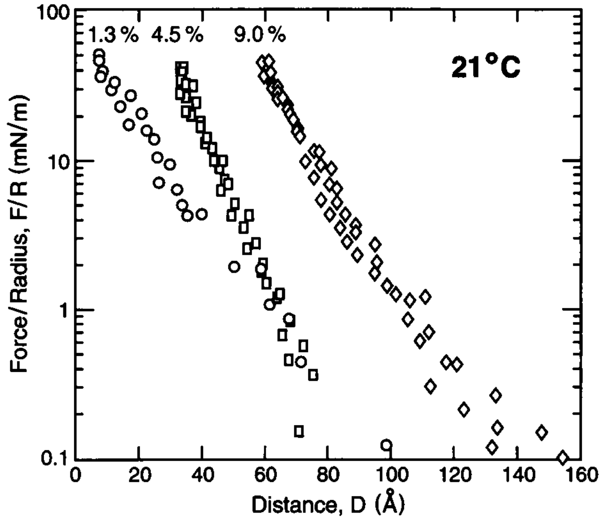

FIGURE 8 Steric force-distance profiles as a function of DSPE-EO$_{45}$ surface coverage. The steric forces were determined by subtracting the electrostatic double-layer repulsion assuming constant surface charge from the measured force profiles (Fig. 7).

TABLE 3 Polymer layer specifications

Surface coverage of polymer (% DSPE-EO$_{45}$)	PEO chain* extension L	Packing area per molecule	Packing area per PEO chain Γ	Distance between grafting sites s
	Å	Å^2	Å^2	Å
1.3	35	43	3300	33
4.5	35–40	43	960	18
9.0	65–75	43	480	12

* Determined from range of forces in Fig. 8. Theoretically, R_F = 35Å, R_g = 23Å.

Temperature dependence

Because of the in vivo application of this system, all polymer surface coverages were investigated for changes in the interaction profile upon changing from conditions of room temperature (21°C) to close to physiological conditions at 33°C. At these temperatures both DPPE and DSPE remain in the solid gel phase, exhibiting no phase transition or increase in fluidity (Marra, 1985). Increasing the temperature to physiological conditions has three effects: (i) the osmotic force increases, resulting in an increased stretching of the chains, (ii) thermal fluctuations of the chains and lipids increase, and (iii) the solvent becomes poorer with increasing temperature causing chain contraction. However, the polymer's elasticity resists thermal extension and stretching. As

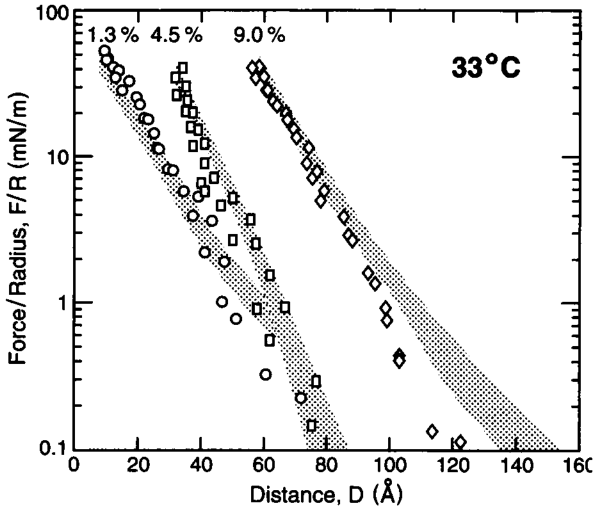

FIGURE 9 Effect of changing temperature from 21°C (*shaded area*) to 33°C (*symbols*) at different DSPE-EO$_{45}$ concentrations.

seen in Fig. 9, these effects apparently cancel each other out or were too small to measure for the lower "mushroom" surface coverages (1.3 and 4.5% DSPE-EO$_{45}$). However, the 9.0% DSPE-EO$_{45}$ "brush" regime does appear to extend slightly less at 33°C. This is also the concentration that should be more sensitive to changes in solvent quality because there is significantly less solvent surrounding the chains as they become compressed. More detailed experiments exploring the effect of solvent quality and brush collapse are underway.

We would also note that at each of the DSPE-EO$_{45}$ grafting densities investigated here, the force curves were reversible and did not show hysteresis (curves not shown). In other surface force studies of adsorbed or physically grafted PEO chains on mica, the force profiles demonstrated significant hysteresis, where the measured repulsion was greater on approach then separation (Klein and Luckham, 1984; Israelachvili et al., 1980; Claesson et al., 1990).

Comparison with theory

Low coverage (1.3%)

A number of theoretical studies have modeled the interaction forces between surfaces with terminally bound sterically stabilizing polymers. One of the first comprehensive models based on the configurational free energy of random flight polymer chains was proposed by Dolan and Edwards (1973). Their model applies to systems with a low surface coverage of polymer where each chain or mushroom interacts with the opposite surface independently of the other chains. Although the random walk model limits the applicability of this theory to theta solvents (water is a good solvent for PEO), this is one of the few theories applicable to the dilute 1.3% DSPE-EO$_{45}$ regime where the chains are noninteracting mushrooms. The Dolan and Edwards equation for the force as a function of distance from about 1 to 8 R_g is approximately given by (Israelachvili, 1991)

$$\frac{F(D)}{R} = 72\pi\Gamma kTe^{-D/R_g} \tag{3}$$

where R_g is the radius of gyration of a random coil in a theta solvent and corresponds to the thickness of the polymer layer extending from the bilayer surface. In most systems it is difficult to know precisely the surface coverage of polymer, Γ. This major drawback is successfully overcome in this study, where the surface coverage was accurately controlled and determined during the LB deposition (see Materials and Methods). Fig. 10 displays the results from fitting the data of Fig. 6 at 1.3% DSPE-EO$_{45}$ to the above equation together with the electrostatic double layer force, assumed to be simply additive with the steric force. As seen, the fit is remarkably good, and it is apparent that this theoretical equation for theta solvents can be applied to this good solvent system. The numerical prefactor, $72\pi\Gamma kT$, is explicitly determined from the experimental data. The only variable in Eq. (3) that was fitted was R_g, the radius of gyration of a random coil in a theta solvent. For the case of a good solvent as we have here, it is more appropriate to use R_F, the Flory radius. For PEO chains of M_r 2000, R_F = 35 Å. The theoretical fit yielded a decay length or polymer layer thickness of 31.2 Å. This value is in very good agreement and as already noted for the area coverage, indicates that the coil extends one Flory radius, as expected from simple scaling concepts. Both the steric and the electrostatic portion of the interaction were fit using two exponential terms. The electrostatic repulsion was determined previously and incorporated directly into the model. This was necessary because of the long range (8 R_F) applicability of the model (Israelachvili, 1991). When the data from 4.5 and 9.0% DSPE-EO$_{45}$ were fit to the Dolan and Edwards expression, the fits were poor and resulted in the wrong trend, i.e., the polymer thickness in both cases was

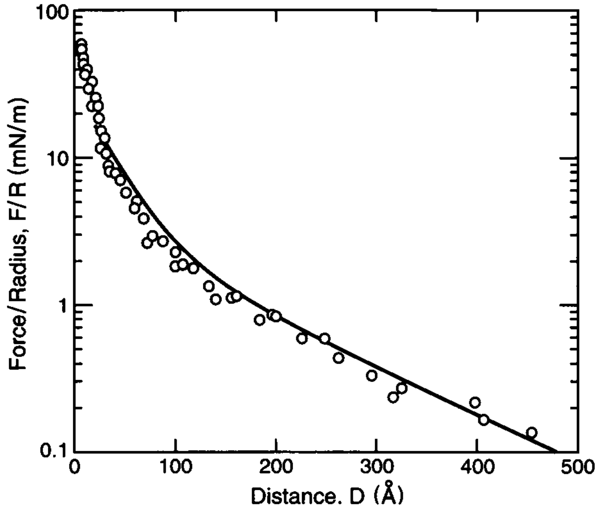

FIGURE 10 Data of the "dilute mushroom" regime of 1.3% DSPE-EO$_{45}$ in Fig. 6 fit to the Dolan and Edwards Equation (3) using Γ = 3300 Å^{2}, R_F = 31 Å, and the values of Table 2 for the double layer force.

calculated to be less than that found for the 1.3%. This was not surprising, considering that these coverages no longer correspond to isolated coils.

High coverage (4.5–9.0%)

For the high coverage regimes, Alexander and de Gennes developed a theory for terminally grafted polymer brushes in good solvents based on scaling arguments (Alexander, 1977; de Gennes, 1981, 1987). The resulting distance dependence of the force contains two terms, an osmotic repulsion between the coils that favors their stretching and an elastic energy of the chains that opposes stretching. For separation distances below twice the thickness of the polymer brush layer, L, the force with distance for two curved cylindrical surfaces of radius R, is described by

$$\frac{F(D)}{R} = \frac{16KT\pi L}{35s^3}\left[7\left(\frac{2L}{D}\right)^{5/4} + 5\left(\frac{D}{2L}\right)^{7/4} - 12\right] \quad \text{for} \quad D < 2L, \tag{4}$$

where the brush thickness is given by

$$L = s\left(\frac{R_F}{s}\right)^{5/3}, \tag{5}$$

where s is the average distance between PEO grafting sites. When Eq. 4 was fit to the experimental force profile of the 9.0% DSPE-EO$_{45}$ brush, allowing only the characteristic brush thickness to vary, the fit was poor. However, scaling arguments do not provide the numerical prefactor. When both the prefactor and the brush thickness were allowed to vary, the fit was reasonable for the model, yielding a brush thickness of 54 Å (Fig. 11). This is less than the experimentally determined thickness of 65–70 Å. However, the experimentally determined thickness is in remarkable agreement with the theoretical prediction of Eq. 5, which for $R_F = 35$ Å, $s = 12$ Å, yields $L = 70$ Å. Additionally, the numerical prefactor was found to be a simple factor of 2, very close to the expected order unity (de Gennes, 1981). Surprisingly, the weakly overlapping mushrooms with 4.5% DSPE-EO$_{45}$ were also well fit by the expression describing the brush regime. When the data for the 1.3% DSPE-EO$_{45}$ dilute regime were fit to the theoretical expression, the fit was poor and unphysical, yielding a larger polymer thickness than for the higher surface coverages of 4.5 and 9.0%. The fitted values for these theoretical models are tabulated in Table 4.

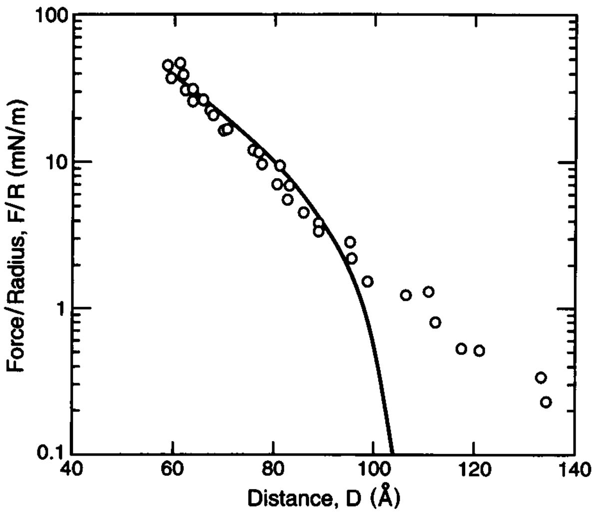

FIGURE 11 Data of the "brush" regime (9.0%) in Fig. 8 fit to the Alexander de Gennes Equation (4) using $S = 12$ Å, $L = 54$ Å.

In summary, the theoretical expressions for force with distance are able to fit the data well in the low coverage regime of 1.3% DSPE-EO$_{45}$ and, when the prefactor is able to vary, in the brush regime of 9.0% and weakly overlapping mushrooms at 4.5% DSPE-EO$_{45}$. Both theoretical equations underestimated the polymer layer thickness. However, more recent self-consistent mean field calculations (Milner et al., 1988) and molecular dynamic simulations (Murat and Grest, 1989) predict a smoothly decaying asymptotic tail of the polymer layer rather than the sharp cut-off of the Alexander de Gennes equation. As seen in Fig. 11, the Alexander de Gennes fit for the force profile decreases too rapidly at large separations and underestimates the tail portion of the polymer layer and, hence, its thickness.

Discussion

The exact basis of the extended circulation times in vivo of liposomes containing lipids with bulky hydrophilic headgroups is still not fully understood. There is considerable debate as to whether the ethylene oxide chains merely provide a steric barrier around the liposome, preventing the close approach of other protein and cellular surfaces in the body or if PEO's particular biocompatibility and chemical inertness also play a significant role (Woodle and Lasic, 1992).

Protein adsorption onto PEO-coated surfaces has been shown to be very low in a number of studies (Golander et al., 1992; Kiss et al., 1987; Mori et al., 1982; K. Nilsson Ekdahl and co-workers, unpublished data). Adsorption of proteins decreases with increasing M$_r$ of the PEO chains up to a limiting value of M$_r$ = 1500, after which, increasing M$_r$ does not further reduce the adsorption, presumably because of a decrease in the grafting density of PEO chains in the steric layer. It would appear that a minimally thick, but dense layer

TABLE 4 Parameters from theoretical equations

Surface coverage of polymer (% DSPE-EO$_{45}$)	Experimental polymer layer thickness*	Model determined thickness	Fitted theoretical thickness
	Å		Å
1.3	35	35ÅD&E*	31.2
4.5	35–45	35Å D&E	9.1
4.5	35–40	35Å AdG	33.8
9	65–70	42Å AdG	54.1

D&E = Dolan and Edwards; AdG = Alexander de Gennes Theory.
* Deduced from the maximum range of the steric forces.

of PEO is necessary to protect the liposome's lipid surface. In this way, proteins and other blood components will not have access to the lipid surface, and the lipid headgroups will be protected from proteins. Moreover, short-ranged van der Waals attraction and longer-ranged electrostatic interactions are dominated by the steric repulsion between the polymer chains as the layers become compressed.

As we have shown, the steric barrier is easily modified by controlling the amount of DSPE-EO_{45} in the bilayer. Based on our LB studies, stable monolayers are formed at the air-water interface with concentrations ranging from about 1 to 10 mol%, and they are easily transferred onto hydrophobic substrates by LB deposition. The lateral interaction of the polymer chains is clearly indicated by the higher surface pressure readings at a given packing area compared with that of pure DSPE. This higher surface pressure manifests itself as a lateral stress on the bilayer. In the case of our supported bilayers, this lateral stress is not large enough to disrupt the bilayer structure. However, free liposomes or vesicles in solution are much more flexible, and the same lateral stresses could increase the area per headgroup or cause more dramatic bulges and buckling of the bilayer surface. Each of these effects would lead to the exposure of hydrophobic groups on the surface, which are ideal sites for protein adsorption. Further, Cevc and Blume (1993) found that vesicle longevity increases and then decreases with the amount of DSPE-EO_{110} incorporated into vesicles, with maximum stability occurring at a coverage of ~5% (about the same surface coverage, when normalized by $\pi R_F^2/A$, as 9% DSPE-EO_{45}). Although they attribute this effect to the suppressed "mobility" of the polymer chains as the concentration of chains increases, it is more likely that the stability of the vesicle bilayers is effected at the higher surface concentrations. Our data show that at concentrations of 9% DSPE-EO_{45} the PEO chains strongly repel each other, producing large destabilizing lateral stresses on the bilayers. Complementary work of D. Needham, T. McIntosh, and K. Hristova (personal communication) using the osmotic stress technique has also indicated that the bilayer structure becomes disrupted at high concentrations of PEO modified lipids. Further, the monolayers do not desorb or change over the time of our experiments (up to 5 days). Based on the extended but finite circulation time of similarly composed liposomes, it would appear that the liposome structure itself rather than the polymeric barrier provided by the PEG chains degrades with time.

Regarding modeling the interaction between short polymer chains or large lipid headgroups, we have shown that simple polymer-based theoretical models of randomly coiled high M_r chains can be invoked to fit quantitatively the interaction forces between surprisingly short PEO chains "terminally grafted" to the fluid bilayer interface. The simplification of a step profile in the density of the chains has been shown to be inconsistent with our experimental data for short polymer chains, but it has also been shown to be inconsistent for longer polymer chains (Taunton et al., 1990). More rigorous calculations by self-consistent mean field and molecular dynamics computer simulations have recently predicted a smoothly decaying asymptotic tail, as seen in the experimental data. The use of such theories may help predict the optimal steric barrier thickness and density to protect in vivo liposomes from degradation.

CONCLUSIONS

Interbilayer interactions are modified greatly by the addition of a small concentration of DSPE-EO_{45}. The PE bilayers no longer adhere because the van der Waals attraction is swamped by the steric repulsion of the polymer chains. These short polymer chains provide a physical barrier or "force buffer" around the bilayer preventing the close approach of other surfaces, the strength and thickness of which was easily manipulated by varying the concentration of the modified DSPE-EO_{45} within the bilayer. This steric barrier correlates directly with the longer in vivo circulation time found for liposomes containing modified lipids with ethylene oxide headgroups. Moreover, the ineffectiveness of liposomes as drug carriers observed at higher concentrations of these bulky lipids corresponds with the onset of large lateral stresses within the bilayer generated because the polymer chains begin to strongly overlap. Finally, two theoretical models developed for long, terminally grafted polymer chains were found to fit the experimental data.

This work was supported by grants from the National Science Foundation (CTS-90-15537) for T.L.K. and from the National Institutes of Health (PHS GM47334) for D.E.L. We thank Phil Pincus for illuminating discussions.

REFERENCES

Alexander, S. 1977. Adsorption of chain molecules with a polar head: a scaling description. *J. Physique (Paris).* 38:983–987.

Allen, T., C. Hansen, F. Martin, C. Redmann, and A. Yau-Young. 1991a. Liposomes containing synthetic lipid derivatives of poly(ethylene glycol) show prolonged circulation half-lives in vivo. *Biochim. Biophys. Acta.* 1066:29–36.

Allen, T., G. Austen, A. Chonn, L. Lin, and K. Lee. 1991b. Uptake of liposomes by cultured mouse bone marrow macrophages: influence of liposome composition and size. *Biochim. Biophys. Acta.* 1061:56–64.

Arnold, K., A Herrmann, L. Pratsch, and K. Gawrisch. 1985. The dielectric properties of aqueous solutions of poly(ethylene glycol) and their influence on membrane structure. *Biochim. Biophys. Acta.* 815:515–518.

Bailey, F., and J. Koleske. 1990. Configuration and hydrodynamic properties of the polyoxyethylene chain in solution. *In* Nonionic Surfactants, Vol. 23. M. Schick, editor. Marcel Dekker, New York. 927–969.

Blume, G., and G. Cevc. 1990. Liposomes for the sustained drug release in vivo. *Biochim. Biophys. Acta.* 1029:91–97.

Blume, G., and G. Cevc. 1993. Molecular mechanism of the lipid vesicle longevity in vivo. *Biochim. Biophys. Acta.* 1146:157–168.

Chen, S., and E. Shen. 1990. Interparticle correlations in concentrated charged colloidal solutions—theory and experiment. *In* Micellar Solutions and Microemulsions. S. Chen and R. Rajagopalan, editors. Springer-Verlag, New York. 3–27.

Claesson, P., D. Cho, C. Golander, E. Kiss, and J. Parker. 1990. Functionalized mica surfaces obtained by a cold plasma process. *Progr. Colloid Polymer Sci.* 82:330–336.

de Gennes, P. 1981. Polymer solutions near an interface. 1. Adsorption and depletion layers. *Macromolecules.* 14:1637–1644.

de Gennes, P. 1987. Polymers at an interface: a simplified view. *Adv. Colloid Interface Sci.* 27:189–209.

de Gennes, P. G. 1979. Scaling Concepts in Polymer Physics. Cornell University Press, New York. 324 pp.

Dolan, A., and F. Edwards. 1974. Theory of the stabilization of colloids by adsorbed polymer. *Proc. Royal Soc. Lond. A.* 337:509–516.

Gaines, G. 1969. Insoluble Monolayers at Liquid-Gas Interfaces, John Wiley & Sons, Inc., New York. 386 pp.

Glowinkowski, S., K. Jurga, and Z. Pajak. 1981. NMR study of molecular motion in poly(ethylene oxide). *Polymer Bull.* 5:271–275.

Golander, C.-G., J. Herron, K. Lim, P. Claesson, P. Stenius, and J. Andrade. 1992. Properties of immobilized PEG films and the interaction with proteins. *In* Poly(ethylene Glycol) Chemistry: Biotechnical and Biomedical Applications. J. M. Harris, editor. Plenum Press, New York. 221–245.

Grabbe, A. 1993. Double layer interactions between silylated silica surfaces. *Langmuir* 9:797–801.

Israelachvili, J. 1973. Thin film studies using multiple beam interferometry. *J. Colloid Interface Sci.* 44:259–272.

Israelachvili, J. 1991. Intermolecular and Surface Forces. Academic Press Limited, London. 450 pp.

Israelachvili, J., and Adams, G. 1978. Measurement of forces between two mica surfaces in aqueous electrolyte solutions in the range 0–100 nm. *J. Chem. Soc. Faraday Trans. I.* 74:975–1001.

Israelachvili, J. N., R. K. Tandon, and L. R. White. 1980. Measurement of forces between two mica surfaces in aqueous poly(ethylene oxide) solutions. *J. Colloid Interface Sci.* 78:430–443.

Kiss E., C.-G. Golander, and J. Ericksson. 1987. Surface grafting of poly ethylene oxide optimized by means of ESCA. *Progr. Colloid Polymer Sci.* 74:113–119.

Kjellander, R., and E. Florin.1981. Water structure and changes in thermal stability of the system poly(ethylene oxide)-water. *J. Chem. Soc. Faraday Trans. I.* 77:2053–2077.

Klein, J., and P. Luckham. 1984. Forces between two adsorbed poly(ethylene oxide) layers in a good aqueous solvent in the range 0–150 nm. *Macromolecules.* 17:1041–1048.

Klibanov, A., K. Maruyama, V. Torchilin, and L. Huang. 1990. Amphipathic poly(ethyleneglycol) effectively prolong the circulation time of liposomes. *FEBS Lett.* 268:235–237.

Koenig, J., and A. Angood. 1970. Raman spectra of poly(ethylene glycols) in solution. *J. Polymer Sci. Part A-2.* 8:1787–1796.

Lasic, D., F. Martin, A. Gabizon, S. Huang, and D. Papahadjopoulos. 1991. Sterically stabilized liposomes: a hypothesis on the molecular origin of the extended circulation times. *Biochim. Biophys. Acta.* 1070:187–192.

Leckband, D., C. Helm, and J. Israelachvili. 1993. The role of calcium in the adhesion and fusion of bilayers. *Biochemistry.* 32:1127–1140.

Liu, K., and J. Parsons. 1969. Solvent effects on the preferred conformation of poly(ethylene glycols). *Macromolecules.* 2:529–533.

Maconnachie, A., P. Vasudevan, and G. Allen. 1978. Molecular dynamics of poly(ethylene oxide) in concentrated solutions. *Polymer.* 19:33–38.

Marra, J., and J. Israelachvili. 1985. Direct measurements of forces between phosphatidylcholine and phosphatidylethanolamine bilayers in aqueous electrolyte solutions. *Biochemistry.* 24:4608–4618.

Marra, J., Ph. D. Thesis. 1985. Forces between Bilayers. Australian National University, Canberra, Australia.

Milner, S., T. Witten, and M. Cates. 1988. Theory of the grafted polymer brush. *Macromolecules.* 21:2610–2619.

Mori, Y., S. Nagaoka, H. Takiuchi, T. Kikuchi, N. Noguchi, H. Tanzawa, and Y. Noishiki. 1982. Poly tetranfluoroethylene grafts coated with ULTI carbon. *Trans. Am. Soc. Artif. Internal Organs.* 28:459–463.

Murat, M., and G. S. Grest. 1989. Structure of a grafted polymer brush: a molecular dynamics simulation. *Macromolecules.* 22:4054–4059.

Needham, D., K. Hristova, T. McIntosh, M. Dewhirst, N. Wu, and D. Lasic. 1992a. Polymer-grafted liposomes: physical basis for the "stealth" property. *J. Liposome Res.* 2:411–430.

Needham, D., T. McIntosh, and D. Lasic. 1992b. Repulsive interactions and mechanical stability of polymer-grafted lipid membranes. *Biochim. Biophys. Acta.* 1108:40–48.

Papahadjopoulos, D., T. Allen, A. Gabizon, E. Mayhew, K. Matthay, S. Huang, K. Lee, M. Woodle, D. Lasic, C. Redemann, and F. Martin. 1991. Sterically stabilized liposomes: Improvements in pharmacokinetics and antitumor therapeutic efficacy. *Proc. Natl. Acad. Sci. USA.* 88: 11460–11464.

Parker, J., D. Cho, and P. Claesson. 1989. Plasma modification of mica: forces between fluorocarbon surfaces in water and a nonpolar liquid. *J. Phys. Chem.* 93:6121–6125.

Small, D. M. 1967. Phase equilibria and structure of dry and hydrated egg lecithin. *J. Lipid Res.* 8:551–557.

Tanford, C. 1972. Micelle shape and size. *J. Phys. Chem.* 93:917–922.

Taunton, H., C. Toprakcioglu, L. Fetters, and J. Klein. 1990. Interactions between surfaces bearing end-adsorbed chains in a good solvent. *Macromolecules.* 23:571–580.

Woodle, M., and D. Lasic. 1992. Sterically stabilized liposomes. *Biochim. Biophys. Acta.* 1113:171–199.